JCAMECH

Vol. 48, No. 1, June 2017, pp 15-26
DOI: 10.22059/jcamech.2017.233643.144

Transient thermoelastic analysis of FGM rotating thick cylindrical pressure vessels under arbitrary boundary and initial conditions

Azam Afshin[1], Mohammad Zamani Nejad[1,*], Kia Dastani[2]

[1] *Mechanical Engineering Department, Yasouj University, P. O. Box: 75914-353, Yasouj, Iran.*

[2] *School of Mechanical Engineering, University of Tehran, Tehran, Iran.*

Received: 20 May. 2017, Accepted: 25 June. 2017

Abstract

Assuming arbitrary boundary and initial conditions, a transient thermo-elastic analysis of a rotating thick cylindrical pressure vessel made of functionally graded material (FGM) subjected to axisymmetric mechanical and transient thermal loads is presented. Time-dependent thermal and mechanical boundary conditions are assumed to act on the boundaries of the vessel. Material properties of the vessel are assumed to be graded in the radial direction according to a power law function. The Poisson's ratio is assumed to be constant. Method of separation of variables has been used to analytically calculate the time dependent temperature distribution as a function of radial direction. In a case study, the distribution of radial and hoop stresses along the thickness is derived and plotted. In order to validate the model, the analytical results have been compared with finite element method modeling results presented in literature. Any arbitrary boundary and initial conditions can be handled using the equations derived in the present research. In order to investigate the inhomogeneity effect on time dependent stress distribution and displacements, values of the parameters have been set arbitrary in the present study. To the best of the authors' knowledge, in previous researches, transient thermo-elastic analysis of thick cylindrical FGM pressure vessels is investigated by numerical methods, while in the present research, an exact solution is derived for the same problem.

Keywords: Thick cylindrical pressure vessel, functionally graded material (FGM), Transient thermo-elastic

1. Introduction

Functionally graded materials (FGMs) are a new generation of composite materials first introduced by a group of Japanese scientists in 1984 [1,2]. From viewpoints of solid mechanics, the FGMs are heterogeneous composite materials wherein the volume fractions of constituent materials vary continuously in some specific directions, such as thickness direction [3]. The corresponding author have

* Corresponding Author. Tel.: +98 7433221711; fax.: +98 7433221711
E-mail address: m_zamani@yu.ac.ir , m.zamani.n@gmail.com (M.Z. Nejad)

published a number of papers addressing various aspects of FGM in recent years [4-10].

Scientific literature is filled with hundreds of works dealing with various aspects of functionally graded materials such as heat transfer [11,12], statically and dynamically stress and deformation analysis [13,14], optimization of FGM [15-17] and manufacturing and design issues and fatigue problems [18-21]. Also functionally graded materials have been used for biomedical applications in recent year due to their ability to satisfy biomaterials requirements such as nontoxicity, corrosion resistance, strength and etc. [22].

In the present research transient thermoelastic analysis of a FGM pressure vessel is carried out. In a research, transient thermoelastic analysis of pressurized thick spheres subjected to arbitrary boundary and initial conditions has been done by Mohammadi et al [23]. Using a numerical method, Han et al. presented the displacement response of FGM shells excited by impact loads [24]. Kim and Noda studied the unsteady-state thermal stress of FGM circular hollow cylinders by using of Green's function method [25]. Chen and Awaji analyzed the thermal stress under thermal shock and residual stress arising from the fabrication process in a hollow cylinder of Functionally graded materials (FGMs) [26]. Liew et al. presented an analytical model for the thermomechanical behavior of FG hollow circular cylinders under the effect of an arbitrary steady state or transient temperature field [27]. Ootao and Tanigawa theoretically studied the transient thermoelastic behavior of a FGM plate [28]. They developed a solution for three-dimensional transient thermal stress of a FGM rectangular plate subjected to a nonuniform heat supply. They assumed that thermal and thermoelastic constants such as the thermal conductivity, the coefficient of linear thermal expansion and Young's modulus are exponential functions of the thickness direction. Heydarpour and Aghdam numerically studied the transient thermoelastic behavior of rotating functionally graded (FG) truncated conical shells subjected to thermal shock [29]. They employed the generalized coupled thermoelasticity based on the Lord–Shulman (L-S) theory. Also they applied different boundary conditions. Mishra et al. analytically studied the force vibration on nonhomogeneous thermoelastic thin FGM annular disk under the application of dynamic pressure by applying the generalized theory of thermoelasticity with one relaxation time [30]. Ghannad and yaghoobi studied steady state thermo-elastic response of axisymmetric FGM cylinder subjected to pressure and external heat flux [31]. They calculated the displacement using first order shear deformation theory. In a research, nonlinear transient thermoelastic analysis of a 2D-FGM thick hollow cylinder is carried out by Najibi and Talebitooti [32]. They also developed a new material model for functionally graded materials based on Mori-Tanaka scheme. By using analytical method, Hosseini et al. studied transient heat conduction in a cylindrical shell of functionally graded material in axisymmetric conditions [33]. Jabbari et al. presented a direct method of solution to obtain the transient mechanical and thermal stresses in a functionally graded hollow cylinder with heat source [34]. Shariyat investigated the nonlinear transient heat transfer and thermoelastic behaviors of the thick-walled FGM cylinders [35]. By using the Hermitian transfinite element method, Azadi and Azadi analyzed nonlinear transient heat transfer and thermoelastic stress of a thick-walled FGM cylinder with temperature dependent materials [36].

In the present research transient thermoelastic analysis of a cylindrical pressure vessel made of a functionally graded material is carried out. The pressure vessel is assumed to be subjected to axisymmetric mechanical and transient thermal loads. In this study an exact solution of mentioned problem is presented which can handle any arbitrary boundary and initial conditions. The results obtained in the present research have been validated by those obtained using numerical methods which are presented in literature.

2. Problem formulation

2.1. *Heat conduction problem*

Here we consider a FGM hollow cylinder which its inner radius is r_i and the outer radius r_o. The material properties assumed that radially dependent as follow:

$$k(r)=k_i\left(\frac{r}{r_i}\right)^{m_5},\ \rho(r)=\rho_i\left(\frac{r}{r_i}\right)^{m_3},\ c(r)=c_i\left(\frac{r}{r_i}\right)^{m_4} \tag{1}$$

In above relations $k(r)$ is thermal conductivity, $\rho(r)$ is density and $c(r)$ is heat capacity. m_3, m_4 and m_5 are the inhomogeneity constants determined empirically, and ρ_i, c_i and k_i are materials properties at inner surface of the cylinder.

In the absence of heat source, the governing equation of one dimensional heat conduction for the case of an axisymmetric hollow cylinder can be written as Eq. 2.

$$\frac{\partial^2 T}{\partial r^2}+\frac{1}{r}\left(m_5+1\right)\frac{\partial T}{\partial r}=\frac{\rho_i c_i}{k_i}\left(\frac{r}{r_i}\right)^{m_3+m_4-m_5}\frac{\partial T}{\partial t} \qquad (2)$$

where $T\left(r,t\right)$ is the temperature distribution which varies over time and thickness direction. The boundary and initial conditions are as follow:

$$B.C.\ :\ \begin{cases} C_{11}T\left(r_i,t\right)+C_{12}\left.\dfrac{\partial T}{\partial r}\right|_{r=r_i}=g_1 \\ C_{21}T\left(r_o,t\right)+C_{22}\left.\dfrac{\partial T}{\partial r}\right|_{r=r_o}=g_2 \end{cases} \qquad (3)$$

$$I.C.\ :\ T\left(r,0\right)=T_i\left(r\right)$$

In above relations, constants $C_{ij}\left(i,j=1,2\right)$ and $g_i\left(i=1,2\right)$ depend on thermal boundary conditions and $T_i\left(r\right)$ is the initial temperature distribution in the cylinder. Under the considered boundary conditions, the solution of Eq. 2 can be obtained as Eq. 4.

$$T\left(r,t\right)=T_s\left(r\right)+T_h\left(r,t\right) \qquad (4)$$

The general solution of Eq. 2 is sum of the general solution $T_s\left(r\right)$ of related homogeneous equation with nonhomogeneous boundary conditions as follow:

$$\frac{\partial^2 T_s}{\partial r^2}+\frac{1}{r}\left(m_5+1\right)\frac{\partial T_s}{\partial r}=0 \qquad (5\text{-a})$$

$$B.C.\ :\ \begin{cases} C_{11}T_s\left(r_i,t\right)+C_{12}\left.\dfrac{\partial T_s}{\partial r}\right|_{r=r_i}=g_1 \\ C_{21}T_s\left(r_o,t\right)+C_{22}\left.\dfrac{\partial T_s}{\partial r}\right|_{r=r_o}=g_2 \end{cases} \qquad (5\text{-b})$$

And solution $T_h\left(r,t\right)$ of nonhomogeneous equation with homogeneous boundary conditions as follow:

$$\frac{\partial^2 T_h}{\partial r^2}+\frac{\left(m_5+1\right)}{r}\frac{\partial T_h}{\partial r}=\frac{\rho_i c_i}{k_i}\left(\frac{r}{r_i}\right)^{m_3+m_4-m_5}\frac{\partial T_h}{\partial t} \qquad (6\text{-a})$$

$$B.C.\ :\ \begin{cases} C_{11}T_h\left(r_i,t\right)+C_{12}\left.\dfrac{\partial T_h}{\partial r}\right|_{r=r_i}=0 \\ C_{21}T_h\left(r_o,t\right)+C_{22}\left.\dfrac{\partial T_h}{\partial r}\right|_{r=r_o}=0 \end{cases} \qquad (6\text{-b})$$

$$I.C.\ :\ T_h\left(r,0\right)=T_i\left(r\right)-T_s\left(r\right)$$

The Eq. (5) is Euler Equation and for $m_5\neq 0$, the solution of this yield:

$$T_s=C_1 r^{-m_5}+C_2 \qquad (7)$$

Applying the boundary conditions of Eq. 5-b, constants C_1 and C_2 can be obtained as follow:

$$C_1=\frac{\left(C_{21}g_1-C_{11}g_2\right)}{\left\{\begin{array}{l} C_{21}r_i^{-m_5}\left(C_{11}-\dfrac{m_5}{r_i}C_{12}\right) \\ -C_{11}r_o^{-m_5}\left(C_{21}-\dfrac{m_5}{r_o}C_{22}\right)\end{array}\right\}} \qquad (8\text{-a})$$

$$C_2=\frac{1}{C_{11}}\left(g_1-C_1 r_i^{-m_5}\left(C_{11}-\frac{m_5}{r_i}C_{12}\right)\right) \qquad (8\text{-b})$$

Also the constant C_2 can be expressed as Eq. 9.

$$C_2=\frac{1}{C_{21}}\left(g_2-C_1 r_o^{-m_5}\left(C_{21}-\frac{m_5}{r_o}C_{22}\right)\right) \qquad (9)$$

The solution of Eq. 6 can be obtained using the method of separation of variables, generalized Bessel function and Eigen-function method as:

$$T_h\left(r,t\right)=\sum_{n=1}^{\infty}C_n f\left(r,\lambda_n\right)e^{-\kappa_i t\lambda_n^2},\kappa_i=\frac{k_i}{\rho_i c_i}r_i^{m_3+m_4-m_5} \qquad (10)$$

In which $f\left(r,\lambda_n\right)$ is Eigen function and is expressed as Eq. 11.

$$f\left(r,\lambda_n\right)=r^{\frac{-m_5}{2}}\left(AJ_p\left(\lambda_n\frac{r^e}{e}\right)+BJ_{-p}\left(\lambda_n\frac{r^e}{e}\right)\right) \qquad (11)$$

Where $p=\dfrac{m_5}{2e}$, $e=\dfrac{\left(m_3+m_4-m_5+2\right)}{2}$, J_p and J_{-p} are Bessel functions of the first kind and of order p, $-p$ respectively. Constants A and B are defined as:

$$A = J_{-p}\left(\lambda_n \frac{r_i^e}{e}\right)\left(C_{11} - C_{12}\frac{m_5}{r_i}\right) - C_{12}\lambda_n r_i^{e-1} J_{-p+1}\left(\lambda_n \frac{r_i^e}{e}\right),\ B = -C_{11}J_p\left(\lambda_n \frac{r_i^e}{e}\right) + C_{12}\lambda_n r_i^{e-1} J_{p+1}\left(\lambda_n \frac{r_i^e}{e}\right) \tag{12}$$

Also we can express constants A and B as Eq. 13.

$$A = J_{-p}\left(\lambda_n \frac{r_o^e}{e}\right)\left(C_{21} - C_{22}\frac{m_5}{r_o}\right) - C_{22}\lambda_n r_o^{e-1} J_{-p+1}\left(\lambda_n \frac{r_o^e}{e}\right),\quad B = C_{22}\lambda_n r_o^{e-1} J_{p+1}\left(\lambda_n \frac{r_o^e}{e}\right) - C_{21}J_p\left(\lambda_n \frac{r_o^e}{e}\right) \tag{13}$$

in the above equations λ_n are Eigen values which are Eq. 14 positive roots.

$$\begin{aligned}&\left\{C_{11}J_p\left(\lambda_n \frac{r_i^e}{e}\right) - C_{12}\lambda_n r_i^{e-1} J_{p+1}\left(\lambda_n \frac{r_i^e}{e}\right)\right\} \times \left\{J_{-p}\left(\lambda_n \frac{r_o^e}{e}\right)\left(C_{21} - C_{22}\frac{m_5}{r_o}\right) - C_{22}\lambda_n r_o^{e-1} J_{-p+1}\left(\lambda_n \frac{r_o^e}{e}\right)\right\} \\ &- \left\{C_{21}J_p\left(\lambda_n \frac{r_o^e}{e}\right) - C_{22}\lambda_n r_o^{e-1} J_{p+1}\left(\lambda_n \frac{r_o^e}{e}\right)\right\} \times \left(J_{-p}\left(\lambda_n \frac{r_i^e}{e}\right)\left(C_{11} - C_{12}\frac{m_5}{r_i}\right) - C_{12}\lambda_n r_i^{e-1} J_{-p+1}\left(\lambda_n \frac{r_i^e}{e}\right)\right) = 0\end{aligned} \tag{14}$$

The coefficient C_n is obtained as follow

$$C_n = \frac{1}{\left\| f\left(r,\lambda_n\right)\right\|^2} \times \left(\begin{array}{l} \int_{r_i}^{r_o} r^{m_5+2e-1} T_i\left(r\right) f\left(r,\lambda_n\right) dr \\ -\sum_{k=0}^{\infty} \frac{\left(-1\right)^k}{2e} \left[A\left(\frac{\lambda_n}{2e}\right)^{2k+p} \left(\begin{array}{l} \frac{C_1\left(r_o^{2e(k+1)} - r_i^{2e(k+1)}\right)}{(k+1)!\,\Gamma(k+p+1)} \\ + \frac{C_2\left(r_o^{2e(k+1)+m_5} - r_i^{2e(k+1)+m_5}\right)}{k!\,\Gamma(k+p+2)} \end{array} \right) + B\left(\frac{\lambda_n}{2e}\right)^{2k-p} \left(\begin{array}{l} \frac{C_1\left(r_o^{2e(k+1)-m_5} - r_i^{2e(k+1)-m_5}\right)}{k!\,\Gamma(k-p+2)} \\ + \frac{C_2\left(r_o^{2e(k+1)} - r_i^{2e(k+1)}\right)}{(k+1)!\,\Gamma(k-p+1)} \end{array} \right) \right] \end{array} \right) \tag{15}$$

The term $\left\| f\left(r,\lambda_n\right)\right\|^2$ is the norm of Eigen function and is obtained as Eq. 16.

$$\begin{aligned}&\left\| f\left(r,\lambda_n\right)\right\|^2 = \int_{r_i}^{r_o} r^{m_5+2e-1} f^2\left(r,\lambda_n\right) dr = \frac{r_o^{2e}}{2e}\left[\left(AJ_p\left(\lambda_n \frac{r_o^e}{e}\right) + BJ_{-p}\left(\lambda_n \frac{r_o^e}{e}\right)\right)^2 + \left(AJ_{p+1}\left(\lambda_n \frac{r_o^e}{e}\right) + BJ_{-p+1}\left(\lambda_n \frac{r_o^e}{e}\right)\right)^2\right. \\ &\left. - \frac{2pe}{\lambda_n r_o^e}\left(A^2 J_p\left(\lambda_n \frac{r_o^e}{e}\right) J_{p+1}\left(\lambda_n \frac{r_o^e}{e}\right) - B^2 J_{-p}\left(\lambda_n \frac{r_o^e}{e}\right) J_{-p+1}\left(\lambda_n \frac{r_o^e}{e}\right)\right)\right] - \frac{r_i^{2e}}{2e}\left[\left(AJ_p\left(\lambda_n \frac{r_i^e}{e}\right) + BJ_{-p}\left(\lambda_n \frac{r_i^e}{e}\right)\right)^2\right. \\ &\left. + \left(AJ_{p+1}\left(\lambda_n \frac{r_i^e}{e}\right) + BJ_{-p+1}\left(\lambda_n \frac{r_i^e}{e}\right)\right)^2 - \frac{2pe}{\lambda_n r_i^e}\left[\begin{array}{l} A^2 J_p\left(\lambda_n \frac{r_i^e}{e}\right) J_{p+1}\left(\lambda_n \frac{r_i^e}{e}\right) \\ -B^2 J_{-p}\left(\lambda_n \frac{r_i^e}{e}\right) J_{-p+1}\left(\lambda_n \frac{r_i^e}{e}\right) \end{array}\right]\right.\end{aligned} \tag{16}$$

in which r^{m_5+2e-1} is weight function. Thus temperature distribution is written as Eq. 17.

$$T\left(r,t\right) = T_s\left(r\right) + \sum_{n=1}^{\infty} C_n f\left(r,\lambda_n\right) e^{-\kappa_i t \lambda_n^2} \tag{17}$$

2.2. *Thermoelastic analysis*

Here we consider that the FGM hollow cylinder rotates about its central axis at a constant angular velocity ω For the case of axisymmetric problem, circumferential and radial strains $(\varepsilon_{rr}, \varepsilon_{\theta\theta})$ can be expressed in terms of cylindrical coordinates (r, θ, z) as Eq. 18. The only non-zero component of the displacement is radial displacement u_r, which is dependent only on radial coordinate r. The Poisson's ratio ν is assumed to be constants and the coefficient of linear thermal expansion α and The Young's modulus E are assumed to be graded in the radial direction according to a power law function as Eq. 19.

$$\varepsilon_{rr} = \frac{\partial u_r}{\partial r}, \varepsilon_{\theta\theta} = \frac{u_r}{r} \tag{18}$$

$$E(r) = E_i \left(\frac{r}{r_i}\right)^{m_1} \alpha(r) = \alpha_i \left(\frac{r}{r_i}\right)^{m_2} \tag{19}$$

where m_1 and m_2 are the inhomogeneity constants that determined empirically and E_i and α_i are properties at inner surface of the hollow cylinder. Substituting Eq. 18 and Eq. 19 into thermoelastic constitutive relations for plane- strain problems yields:

$$\sigma_{rr} = \frac{E_i}{(1+\nu)(1-2\nu)}\left(\frac{r}{r_i}\right)^{m_1}\left((1-\nu)\frac{\partial u_r}{\partial r} + \nu\frac{u_r}{r} - (1+\nu)\alpha_i\left(\frac{r}{r_i}\right)^{m_2} T\right) \tag{20-a}$$

$$\sigma_{\theta\theta} = \frac{E_i}{(1+\nu)(1-2\nu)}\left(\frac{r}{r_i}\right)^{m_1}\left((1-\nu)\frac{u_r}{r} + \nu\frac{\partial u_r}{\partial r} - (1+\nu)\alpha_i \times \left(\frac{r}{r_i}\right)^{m_2} T\right) \tag{20-b}$$

$$\sigma_{zz} = \frac{E_i}{(1+\nu)(1-2\nu)}\left(\frac{r}{r_i}\right)^{m_1}\left(\nu\left(\frac{u_r}{r} + \frac{\partial u_r}{\partial r}\right) - (1+\nu)\times\alpha_i\left(\frac{r}{r_i}\right)^{m_2} T\right) \tag{20-c}$$

In the above relations $\sigma_{rr}, \sigma_{\theta\theta}, \sigma_{zz}$ are radial, hoop and axial components of stress. T is the temperature difference as $T = T(r,t) - T_0$ in which T_0 is the ambient temperature which is set to zero in the present study.

Assuming body forces are zero, the equilibrium equation of the hollow cylinder rotates at the angular velocity ω can be written as Eq. 21.

$$\frac{\partial \sigma_{rr}}{\partial r} + \frac{\sigma_{rr} - \sigma_{\theta\theta}}{r} = -\rho r \omega^2 \tag{21}$$

Substituting Eq. 20 in Eq. 21 gives:

$$\frac{\partial^2 u_r}{\partial r^2} + \frac{1}{r}\frac{\partial u_r}{\partial r}(m_1+1) + \frac{u_r}{r^2}\left(\frac{\nu m_1}{1-\nu} - 1\right) - \alpha_i\left(\frac{r}{r_i}\right)^{m_2}\frac{1+\nu}{1-\nu}\left(\frac{\partial T}{\partial r} + \frac{(m_1+m_2)}{r}T\right)$$

$$= -\frac{\rho_i(1+\nu)(1-2\nu)}{(1-\nu)E_i}\omega^2\frac{r^{1+m_3-m_1}}{r_i^{m_3-m_1}} \tag{22}$$

The solution of Eq. 22 can be obtained as Eq.23.

$$u_r(r,t) = r^{\beta_1}\left(C_1^* + \xi_1(r,t)\right) + r^{\beta_2}\left(C_2^* + \xi_2(r,t)\right) \tag{23}$$

In which

$$\beta_1 = \frac{-m_1 + \sqrt{\left(m_1^2 - 4\left(\frac{\nu m_1}{1-\nu} - 1\right)\right)}}{2}$$

$$\beta_2 = \frac{-m_1 - \sqrt{\left(m_1^2 - 4\left(\frac{\nu m_1}{1-\nu} - 1\right)\right)}}{2} \tag{24}$$

and

$$\xi_1(r,t)=-A_2\int_{r_i}^{r}r^{\beta_2+m_3+2}dr-A_1\int_{r_i}^{r}r^{-\beta_1+m_2}\left(r\frac{\partial T}{\partial r}+\begin{pmatrix}m_1\\+m_2\end{pmatrix}T\right)dr=-A_2\int_{r_i}^{r}r^{\beta_2+m_3+2}dr-A_1\int_{r_i}^{r}r^{-\beta_1+m_2}\left[\left(r\frac{\partial T_s(r)}{\partial r}+(m_1+m_2)T_s(r)\right)\right.$$
$$\left.+\sum_{n=1}^{\infty}C_n\left[r\frac{\partial f(r,\lambda_n)}{\partial r}+(m_1+m_2)f(r,\lambda_n)\right]e^{-\lambda_i t\lambda_n^2}\right]dr$$
$$\xi_2(r,t)=A_2\int_{r_i}^{r}r^{\beta_1+m_3+2}dr+A_1\int_{r_i}^{r}r^{-\beta_2+m_2}\left(r\frac{\partial T}{\partial r}+\begin{pmatrix}m_1\\+m_2\end{pmatrix}T\right)dr=A_2\int_{r_i}^{r}r^{\beta_1+m_3+2}dr+A_1\int_{r_i}^{r}r^{-\beta_2+m_2}\left[\left(r\frac{\partial T_s(r)}{\partial r}+(m_1+m_2)T_s(r)\right)\right. \quad (25)$$
$$\left.+\sum_{n=1}^{\infty}C_n\left[r\frac{\partial f(r,\lambda_n)}{\partial r}+(m_1+m_2)f(r,\lambda_n)\right]e^{-\lambda_i t\lambda_n^2}\right]dr$$

Substituting Eq. 23 into Eq. 20 the radial, circumferential and axial stresses of the rotating thick hollow cylinder are obtained as:

$$\sigma_{rr}=\frac{E_i\left(\frac{r}{r_i}\right)^{m_1}}{(1+\nu)(1-2\nu)}\left\{\begin{matrix}(\beta_1(1-\nu)+\nu)\\\times(C_1^*+\xi_1(r,t))r^{\beta_1-1}\end{matrix}+(\beta_2(1-\nu)+\nu)(C_2^*+\xi_2(r,t))r^{\beta_2-1}-(1+\nu)\alpha_i\left(\frac{r}{r_i}\right)^{m_2}T\right\} \quad (26\text{-a})$$

$$\sigma_{\theta\theta}=\frac{E_i\left(\frac{r}{r_i}\right)^{m_1}}{(1+\nu)(1-2\nu)}\left\{\begin{matrix}(1+\nu(\beta_1-1))\\\times(C_1^*+\xi_1(r,t))r^{\beta_1-1}\end{matrix}+(C_2^*+\xi_2(r,t))\times(1+\nu(\beta_2-1))r^{\beta_2-1}-(1+\nu)\alpha_i\left(\frac{r}{r_i}\right)^{m_2}T\right\} \quad (26\text{-b})$$

$$\sigma_{zz}=\frac{E_i\left(\frac{r}{r_i}\right)^{m_1}}{(1+\nu)(1-2\nu)}\left\{\begin{matrix}\nu(\beta_1+1)\\\times(C_1^*+\xi_1(r,t))r^{\beta_1-1}\end{matrix}+\nu(\beta_2+1)(C_2^*+\xi_2(r,t))r^{\beta_2-1}-(1+\nu)\alpha_i\left(\frac{r}{r_i}\right)^{m_2}T\right\} \quad (26\text{-c})$$

By substituting the mechanical boundary conditions which are $\sigma_{rr}=-p_i$ at $r=r_i$ and $\sigma_{rr}=-p_o$ at $r=r_o$ in Eq. 26 coefficients C_1^* and C_2^* can be obtained in terms of mechanical properties and applied pressure as Eq. 27.

$$C_1^*=\frac{r_i^{1-\beta_1}}{(\beta_1(1-\nu)+\nu)\left(\left(\frac{r_o}{r_i}\right)^{\beta_1-1}-\left(\frac{r_o}{r_i}\right)^{\beta_2-1}\right)}\times\left[\frac{(1+\nu)(1-2\nu)}{E_i}\left(P_i\left(\frac{r_o}{r_i}\right)^{\beta_2-1}-P_o\left(\frac{r_o}{r_i}\right)^{-m_1}\right)\right.$$
$$\left.-\left(\begin{matrix}(\beta_1(1-\nu)+\nu)\xi_1(r_o,t)r_o^{\beta_1-1}\\+(\beta_2(1-\nu)+\nu)\xi_2(r_o,t)r_o^{\beta_2-1}\end{matrix}\right)+(1+\nu)\alpha_i\left(T(r_o,t)\left(\frac{r_o}{r_i}\right)^{m_2}-T(r_i,t)\left(\frac{r_o}{r_i}\right)^{\beta_2-1}\right)\right] \quad (27\text{-a})$$

$$C_2^*=\frac{r_i^{1-\beta_2}}{(\beta_2(1-\nu)+\nu)\left(\left(\frac{r_o}{r_i}\right)^{\beta_1-1}-\left(\frac{r_o}{r_i}\right)^{\beta_2-1}\right)}\times\left[\frac{(1+\nu)(1-2\nu)}{E_i}\left(P_o\left(\frac{r_o}{r_i}\right)^{-m_1}-P_i\left(\frac{r_o}{r_i}\right)^{\beta_1-1}\right)\right. \quad (27\text{-b})$$
$$\left.+\left(\begin{matrix}(\beta_1(1-\nu)+\nu)\xi_1(r_o,t)r_o^{\beta_1-1}\\+(\beta_2(1-\nu)+\nu)\xi_2(r_o,t)r_o^{\beta_2-1}\end{matrix}\right)+(1+\nu)\alpha_i\left(T(r_i,t)\left(\frac{r_o}{r_i}\right)^{\beta_1-1}-T(r_o,t)\left(\frac{r_o}{r_i}\right)^{m_2}\right)\right]$$

3. Results and discussions

Consider a hollow cylinder made up of a functionally graded material. The poison's ration is assumed to be constant and it is set to $\nu = 0.3$. Other physical properties are listed in Table 1. The applied pressure on inner surface of cylinder is 70 MPa .

Table 1. physical properties of the hollow FGM cylinder

symbol	value	symbol	value
r_i	0.02 m	c_i	808.3 J/Kg.$^\circ K$
r_o	0.04 m	E_o	200 GPa
E_i	66.2 GPa	ρ_o	7854 Kg/m^3
ρ_i	4410 Kg/m^3	α_o	$1.17\left(10^{-5}\right)1/^\circ\mathrm{C}$
α_i	$1.03\left(10^{-5}\right)1/^\circ\mathrm{C}$	k_o	60.5 W/m.$^\circ$K
k_i	18.1 W/m.$^\circ$K	c_o	434 J/Kg.$^\circ$K

We assume that the temperature is constant over both inner and outer surfaces of the hollow cylinder. Since the initial condition is a linear function of polar coordinate r, thermal boundary conditions can be expressed as Eq. 28.

$$\begin{cases} B.C. \ : \ \begin{cases} T\left(r_i,t\right)=1℃ \\ T\left(r_o,t\right)=2℃ \end{cases} \\ I.C. \ : \ T\left(r,0\right)=20r \end{cases} \qquad (28)$$

In order to validate the solution algorithm, a comparison is performed between the analytical results of presented approach with those calculated by finite element method and presented in literature. In Fig.1 numerical and analytical results of temperature are compared. This figure shows the time dependent temperature at point $r = 0.025\mathrm{m}$ over a course of 20 seconds. Fig. 2 indicates the temperature distribution along thickness of the cylinder at time $t = 5\mathrm{sec}$. Fig.1 and Fig.2 reveal that the analytical results obtained from the present model agree very well with numerical results presented in the literature. Fig. 3 shows the time dependent temperature at different radiuses over a course of 20 seconds. Temperature distribution along the thickness of cylinder is plotted in Fig. 4 at different times.

Radial displacement versus polar coordinate r at time $t = 5\mathrm{sec}$ is plotted in Fig. 5. Distribution of stress components along the thickness of the hollow cylinder at time $t = 5\mathrm{sec}$ is shown in Figures 6 to 8. It is obvious in Fig. 7 that hoop stress increases from inner to outer surface of cylinder. But near the outer surface it decreases.

Fig. 9 shows the radial displacement at point $r = 0.025\mathrm{m}$ over time. Figures 10 to 12 show the radial, hoop and axial components of stress at point $r = 0.025\mathrm{m}$ over a 10 second course. It is obvious that at the beginning, hoop and axial stresses increase and then decrease as time increases. Fig 11 and Fig 12 show that hoop and axial stresses at the initial seconds have maximum values that must be note by designer.

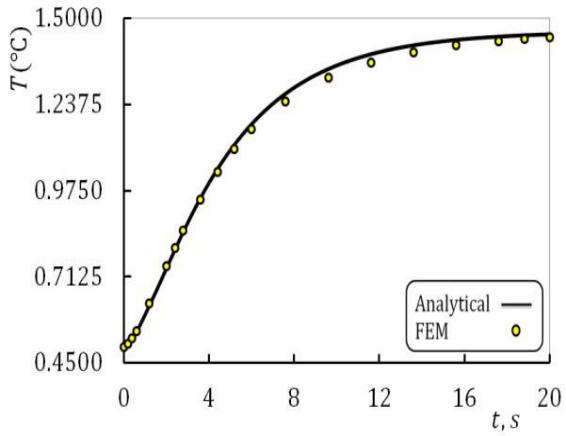

Fig. 1. Temperature at point $r = 0.025\mathrm{m}$.

Figures 13 to 16 indicates the radial displacement and hoop, radial and axial components of stress over time at radiuses $r = 0.025, 0.03, 0.035\mathrm{m}$. Figures 17 to 20 shows the radial displacement versus polar component r and hoop, radial and axial stress distribution along cylinder thickness at different times. These figures verify previous presented results. Fig 19 shows that the hoop stress distribution for different times at a point that $1.25 < r/r_i < 1.75$ is constant and the variation of stress before this point is inverse variation stress after this point. Fig. 21 shows the radial displacement versus polar coordinate r at different angular velocities ω. Radial, hoop and axial stress distribution along the cylinder thickness is plotted in figures 22 to 24 at different angular velocities. These figures show that radial displacement, hoop and axial stresses increase as

increase angular velocity but radial stress decreases, and these variations are very small for radial stress.

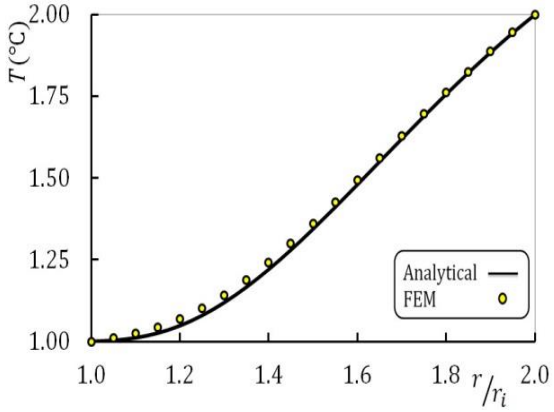

Fig. 2. Temperature distribution along thickness at time $t = 5\text{sec}$.

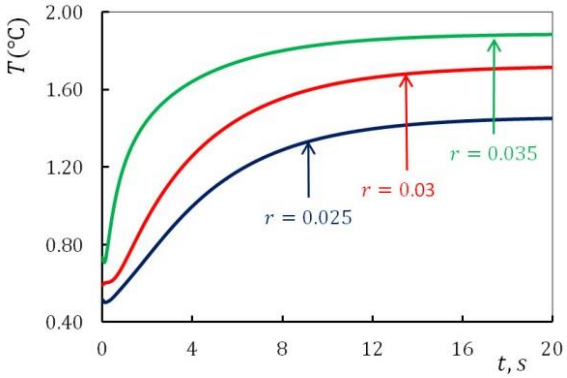

Fig. 3. Comparison of the temperature distribution for different radius.

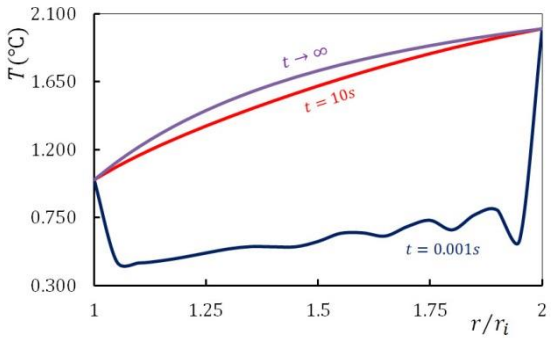

Fig. 4. Comparison of the temperature distribution for different times.

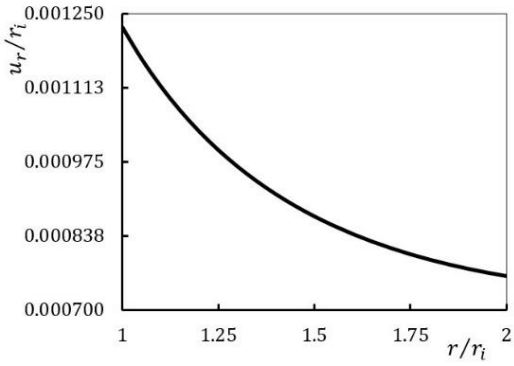

Fig. 5. Radial displacement distribution at time $t = 5\text{sec}$.

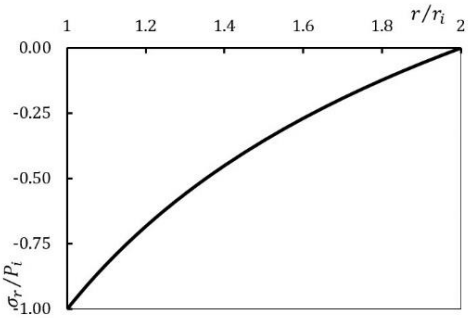

Fig. 6. Radial stress distribution at time $t = 5\text{sec}$.

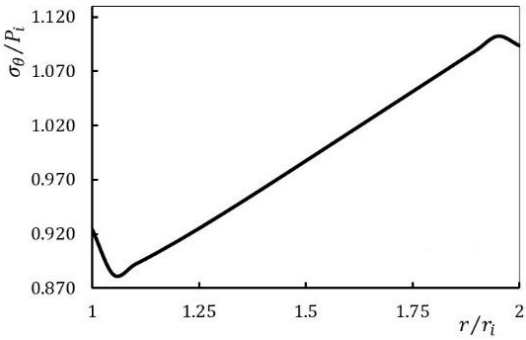

Fig. 7. Hoop stress distribution at time $t = 5\text{sec}$.

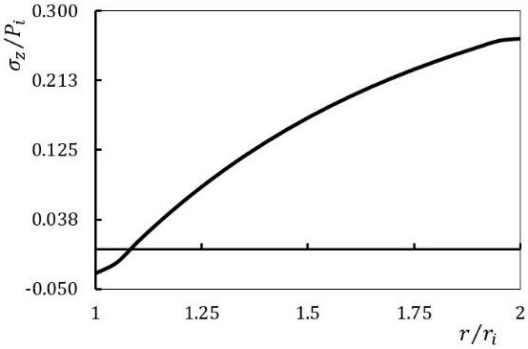

Fig. 8. Axial stress distribution at time $t = 5\text{sec}$.

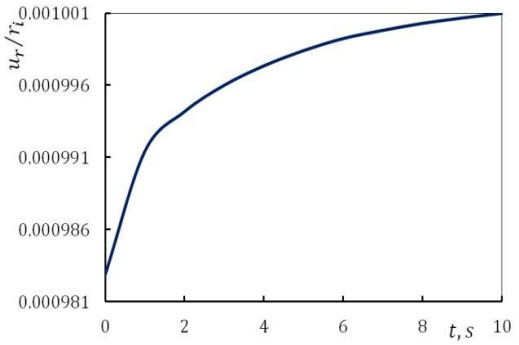

Fig. 9. Radial displacement distribution at point $t = 5\text{sec}$.

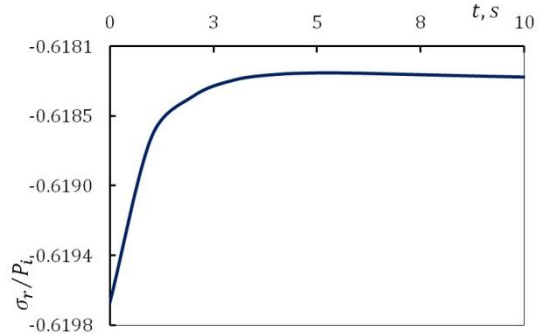

Fig. 10. Radial stress distribution at point $t = 5\text{sec}$.

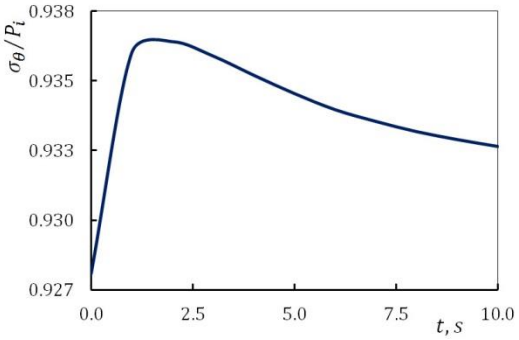

Fig. 11. Hoop stress distribution at point $t = 5\text{sec}$.

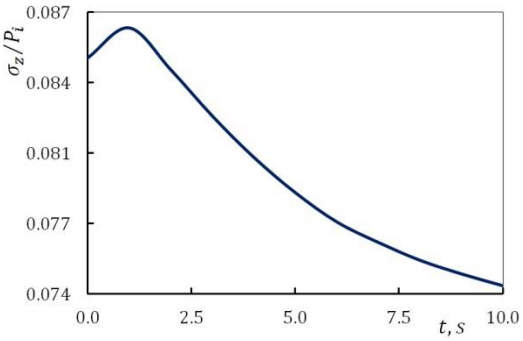

Fig. 12. Axial stress distribution at point $t = 5\text{sec}$.

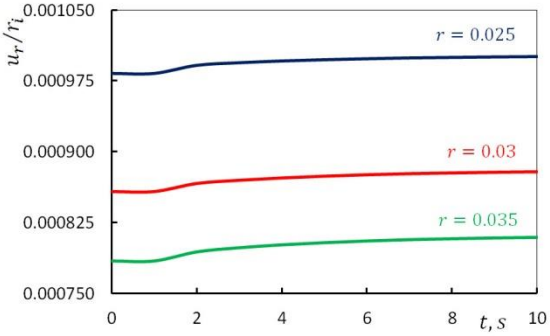

Fig. 13. Comparison of radial displacement distribution at different radius.

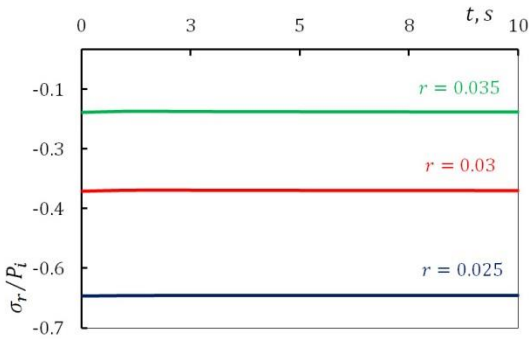

Fig. 14. Comparison of radial stress distribution at different radius.

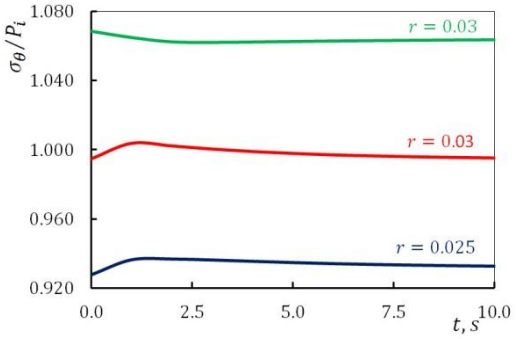

Fig. 15. Comparison of hoop stress distribution at different radius.

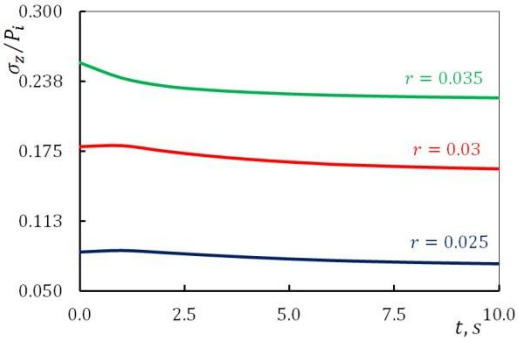

Fig. 16. axial stress distribution at different radius.

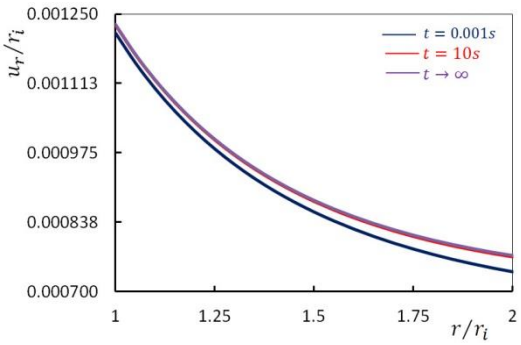

Fig. 17. Comparison radial displacement distribution for different times.

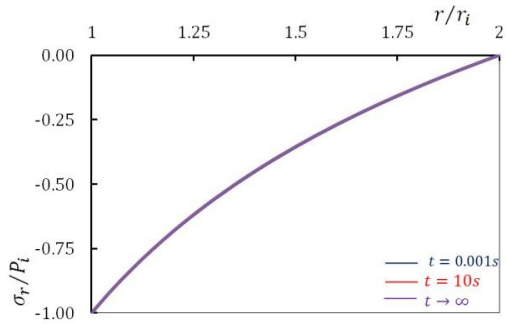

Fig. 18. Comparison of the radial stress distribution for different times.

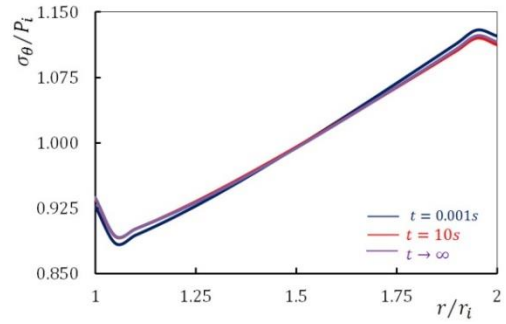

Fig. 19. Comparison hoop stress distribution for different times.

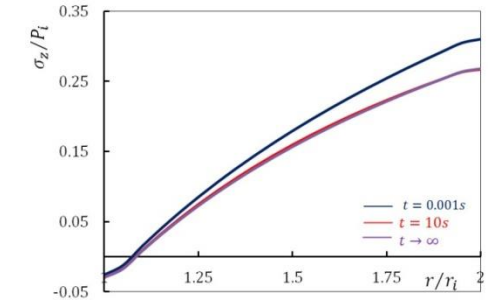

Fig. 20. Comparison the axial stress distribution for different times.

4. Conclusion

In the present article the transient thermoelastic analysis of an axisymmetric hollow cylinder made of a functionally graded material is carried out. Thermal and thermoelastic properties of the material are assumed to be a power function of polar coordinate r. The exact solution of time dependent temperature distribution and transient hoop, radial and axial stress components are obtained under general thermal boundary conditions. By perusing the previous section, it is concluded that hoop and axial stresses increases as radius increase but radial displacement and radial stress decrease; and radial displacement increases as time increase but radial stress decreases; and hoop and axial stresses in the beginning increase and then decrease as time increases. Radial displacement, hoop, and axial stresses increase as angular velocity increase but radial stress decrease and these reductions are very small. Any arbitrary boundary and initial conditions can be handled using the relations presented in this article.

5. References

[1] M. Yamanouchi, M. Koizumi, T. Hirai, I. Shiota, FGM-90, in *Proceeding of*.

[2] A. H. Sofiyev, Influences of shear stresses on the dynamic instability of exponentially graded sandwich cylindrical shells, *Composites Part B: Engineering*, Vol. 77, pp. 349-362, 2015.

[3] M. Ghannad, G. H. Rahimi, M. Z. Nejad, Elastic analysis of pressurized thick cylindrical shells with variable thickness made of functionally graded materials, *Composites Part B: Engineering*, Vol. 45, No. 1, pp. 388-396, 2013.

[4] M. Zamani Nejad, A. Afshin, Transient thermoelastic analysis of pressurized rotating disks subjected to arbitrary boundary and initial conditions, *Chinese Journal of Engineering*, Vol. 2014, 2014.

[5] M. Z. Nejad, M. D. Kashkoli, Time-dependent thermo-creep analysis of rotating FGM thick-walled cylindrical pressure vessels under heat flux, *International Journal of Engineering Science*, Vol. 82, pp. 222-237, 2014.

[6] M. Z. Nejad, A. Rastgoo, A. Hadi, Effect of exponentially-varying properties on displacements and stresses in pressurized functionally graded thick spherical shells with using iterative technique, *Journal of Solid Mechanics*, Vol. 6, No. 4, pp. 366-377, 2014.

[7] M. Z. Nejad, A. Rastgoo, A. Hadi, Exact elasto-plastic analysis of rotating disks made of functionally graded materials,

International Journal of Engineering Science, Vol. 85, pp. 47-57, 2014.

[8] M. Z. Nejad, P. Fatehi, Exact elasto-plastic analysis of rotating thick-walled cylindrical pressure vessels made of functionally graded materials, *International Journal of Engineering Science*, Vol. 86, pp. 26-43, 2015.

[9] M. Jabbari, M. Z. Nejad, M. Ghannad, Thermo-elastic analysis of axially functionally graded rotating thick cylindrical pressure vessels with variable thickness under mechanical loading, *International journal of engineering science*, Vol. 96, pp. 1-18, 2015.

[10] M. Z. Nejad, M. Jabbari, M. Ghannad, Elastic analysis of FGM rotating thick truncated conical shells with axially-varying properties under non-uniform pressure loading, *Composite Structures*, Vol. 122, pp. 561-569, 2015.

[11] Z. H. Jin, An asymptotic solution of temperature field in a strip a functionally graded material, *International communications in heat and mass transfer*, Vol. 29, No. 7, pp. 887-895, 2002.

[12] Y. Ootao, Y. Tanigawa, Transient thermoelastic problem of functionally graded thick strip due to nonuniform heat supply, *Composite Structures*, Vol. 63, No. 2, pp. 139-146, 2004.

[13] N. A. Apetre, B. V. Sankar, D. R. Ambur, Low-velocity impact response of sandwich beams with functionally graded core, *International Journal of Solids and Structures*, Vol. 43, No. 9, pp. 2479-2496, 2006.

[14] B. V. Sankar, An elasticity solution for functionally graded beams, *Composites Science and Technology*, Vol. 61, No. 5, pp. 689-696, 2001.

[15] J. R. Cho, J. T. Oden, Functionally graded material: a parametric study on thermal-stress characteristics using the Crank–Nicolson–Galerkin scheme, *Computer methods in applied mechanics and engineering*, Vol. 188, No. 1, pp. 17-38, 2000.

[16] M. Bahraminasab, B. B. Sahari, K. L. Edwards, F. Farahmand, T. S. Hong, M. Arumugam, A. Jahan, Multi-objective design optimization of functionally graded material for the femoral component of a total knee replacement, *Materials & Design*, Vol. 53, pp. 159-173, 2014.

[17] F. Tornabene, A. Ceruti, Mixed static and dynamic optimization of four-parameter functionally graded completely doubly curved and degenerate shells and panels using GDQ method, *Mathematical Problems in Engineering*, Vol. 2013, 2013.

[18] P. Shanmugavel, G. B. Bhaskar, M. Chandrasekaran, S. P. Srinivasan, Determination of Stress Intensity Factors and Fatigue Characteristics for Aluminium, Aluminium-Alumina Composite Material and Aluminium-Alumina FGM Specimens with Edge Crack by Simulation, *International Journal of Applied Environmental Sciences*, Vol. 9, No. 4, pp. 1759-1768, 2014.

[19] S. Bhattacharya, K. Sharma, V. Sonkar, Numerical simulation of elastic plastic fatigue crack growth in functionally graded material using the extended finite element method, *Mechanics of Advanced Materials and Structures*, pp. 1-14, 2017.

[20] M. Pant, K. Sharma, S. Bhattacharya, Application of EFGM and XFEM for Fatigue Crack growth Analysis of Functionally Graded Materials, *Procedia Engineering*, Vol. 173, pp. 1231-1238, 2017.

[21] K. Sharma, S. Bhattacharya, V. Sonkar, XFEM simulation on Mixed-Mode Fatigue Crack Growth of Functionally Graded Materials, *Journal of Mechanical Engineering and Biomechanics*, Vol. 1, 2016.

[22] B. Gupta, Few Studies on Biomedical Applications of Functionally Graded Material.

[23] S. Mohammadi, M. Z. Nejad, A. Afshin, Transient Thermoelastic Analysis of Pressurized Thick Spheres Subjected to Arbitrary Boundary and Initial Conditions, *Indian Journal of Science and Technology*, Vol. 8, No. 36, 2015.

[24] X. Han, D. Xu, G. R. Liu, Transient responses in a functionally graded cylindrical shell to a point load, *Journal of Sound and Vibration*, Vol. 251, No. 5, pp. 783-805, 2002.

[25] K. S. Kim, N. Noda, Green's function approach to unsteady thermal stresses in an infinite hollow cylinder of functionally graded material, *Acta Mechanica*, Vol. 156, No. 3-4, pp. 145-161, 2002.

[26] C. H. Chen, H. Awaji, Transient and residual stresses in a hollow cylinder of functionally graded materials, in *Proceeding of*, Trans Tech Publ, pp. 665-670.

[27] K. M. Liew, S. Kitipornchai, X. Z. Zhang, C. W. Lim, Analysis of the thermal stress behaviour of functionally graded hollow circular cylinders, *International Journal of Solids and Structures*, Vol. 40, No. 10, pp. 2355-2380, 2003.

[28] Y. Ootao, Y. Tanigawa, Three-dimensional solution for transient thermal stresses of functionally graded rectangular plate due to nonuniform heat supply, *International Journal of Mechanical Sciences*, Vol. 47, No. 11, pp. 1769-1788, 2005.

[29] Y. Heydarpour, M. M. Aghdam, Transient analysis of rotating functionally graded truncated conical shells based on the Lord–Shulman model, *Thin-Walled Structures*, Vol. 104, pp. 168-184, 2016.

[30] K. C. Mishra, J. N. Sharma, P. K. Sharma, Analysis of vibrations in a nonhomogeneous thermoelastic thin annular disk under dynamic pressure, *Mechanics Based Design of Structures and Machines*, Vol. 45, No. 2, pp. 207-218, 2017.

[31] M. Ghannad, M. P. Yaghoobi, 2D thermo elastic behavior of a FG cylinder under thermomechanical loads using a first order temperature theory, *International Journal of Pressure Vessels and Piping*, Vol. 149, pp. 75-92, 2017.

[32] A. Najibi, R. Talebitooti, Nonlinear transient thermo-elastic analysis of a 2D-FGM thick hollow finite length cylinder, *Composites Part B: Engineering*, Vol. 111, pp. 211-227, 2017.

[33] S. M. Hosseini, M. Akhlaghi, M. Shakeri, Transient heat conduction in functionally graded thick hollow cylinders by analytical method, *Heat and Mass Transfer*, Vol. 43, No. 7, pp. 669-675, 2007.

[34] M. Jabbari, A. R. Vaghari, A. Bahtui, M. R. Eslami, Exact solution for asymmetric transient thermal and mechanical stresses in FGM hollow cylinders with heat source, *Structural Engineering and Mechanics*, Vol. 29, No. 5, pp. 551-565, 2008.

[35] M. Shariyat, A rapidly convergent nonlinear transfinite element procedure for transient thermoelastic analysis of temperature-dependent functionally graded cylinders, *Journal of Solid Mechanics*, Vol. 1, No. 4, pp. 313-327, 2009.

[36] M. Azadi, M. Azadi, Nonlinear transient heat transfer and thermoelastic analysis of thick-walled FGM cylinder with temperature-dependent material properties using Hermitian transfinite element, *Journal of Mechanical Science and Technology*, Vol. 23, No. 10, pp. 2635-2644, 2009.